A Sol–Gel Route To Synthesize Monolithic Zinc Oxide Aerogels

Yanping P. Gao, Charlotte N. Sisk, and Louisa J. Hope-Weeks*

Department of Chemistry and Biochemistry, Texas Tech University, Lubbock, Texas 79409

Received July 12, 2007. Revised Manuscript Received September 12, 2007

The epoxide addition sol–gel process is a relatively new route to synthesize transition and main group metal oxide aerogels. Zinc oxide monoliths were obtained by sol–gel processing of an alcoholic zinc nitrate solution with propylene oxide as the gelation initiator. The alcogels were dried either by supercritical CO_2 fluid extraction (aerogel) or by ambient temperature slow evaporation (xerogel). The resulting materials were characterized using powder X-ray diffraction (XRD), high-resolution scanning electron microscopy (HRSEM), nitrogen adsorption/desorption analysis, and photoluminescence (PL). Annealing of the aerogel at low temperatures (below 250 °C) yields a highly crystalline material which exhibits a significant increase in photoluminescence while retaining the inherent characteristics of the original aerogel, including high surface area (>100 m^2/g) and porosity.

Introduction

Zinc oxide (ZnO) materials have received considerable attention due to their distinguished performance in electronics, optics, and photonics.[1–4] From the 1960s, the synthesis of ZnO thin films has been an active field due to their applications as sensors, transducers, and catalysts.[5–8] In the past few decades, developments in nanotechnology and the demonstration of various quantum size effects in nanoscale particles imply that most of the novel devices of the future will be based on properties of nanomaterials. Zinc oxide-based nanoscale materials are highly interesting for a variety of a potential applications since they exhibit both piezoelectric and semiconducting properties with a wide band gap of 3.37 eV and a large exciton binding energy of 60 eV.[1–4,8]

Aerogels are high surface area, low density materials consisting of nanoparticle building blocks networked together to form an open, highly porous structure.[9,10] The inherent characteristics of aerogel-based materials are highly beneficial for a wide variety of actual and potential applications, including absorbing and filtration media, heterogeneous catalysis, thermal insulators, and electrodes for batteries and capacitors.[11–16]

Currently all high surface area materials which incorporate ZnO have utilized traditional alkoxide sol–gel chemistry. Usually silicon alkoxides are used to form stable sol–gel materials which encapsulate ZnO nanoparticles into either an amorphous or semicrystalline SiO_2 matrix.[17–20] To date work in this area has been rather limited, and there have been no reports on the formation of "pure" zinc oxide-based monolithic aerogel materials. Primarily this can be attributed to the instability of zinc alkoxides. Such zinc oxide materials would be highly attractive for a host of catalytic and gas-sensing devices. To this end a new sol–gel technique for the synthesis of transition and main group metal oxide-based porous materials has been reported.[21,22] The method involves the use of simple inorganic salts and epoxides to initiate the sol–gel polymerization reaction. The reaction is driven via deprotonation of the hydrated metal salt by the epoxide. This leads to the subsequent formation of oligomers from the cationic metal species which link together through olation and oxolation to give the metal sol. Subsequent cross-linking of the sol results in the formation of a monolithic gel.[23]

* To whom correspondence should be addressed: e-mail louisa.hope-weeks@ttu.edu; Tel 806-742-4487.

(1) Zhi, M.; Zhu, L.; Ye, Z.; Wang, F.; Zhao, B. *J. Phys. Chem. B* **2005**, *109*, 23930–23934.
(2) Gao, T.; Li, Q.; Wang, T. *Chem. Mater.* **2005**, *17*, 887–892.
(3) Wang, X. D.; Summers, C. J.; Wang, Z. L. *Nano Lett.* **2004**, *4*, 423–426.
(4) Gao, P.; Wang, Z. L. *J. Phys. Chem. B* **2002**, *106*, 12653–12658.
(5) Li, Q.; Kumar, V.; Li, Y.; Zhang, H.; Marks, T. J.; Chang, R. P. H. *Chem. Mater.* **2005**, *17*, 1001–1006.
(6) Schwenzer, B.; Gomm, J. R.; Morse, D. E. *Langmuir* **2006**, *22*, 9829–9831.
(7) Lakshmi, B. B.; Patrissi, C. J.; Martin, C. R. *Chem. Mater.* **1997**, *9*, 2544–2550.
(8) Koch, M. H.; Hartmann, A. J.; Lamb, R. N.; Neuber, M.; Grunze, M. *J. Phys. Chem. B* **1997**, *101*, 8231–8236.
(9) Pierre, A. C.; Pajonk, G. M. *Chem. Rev.* **2002**, *102*, 4243–4265.
(10) Rolison, D. R.; Dunn, B. *J. Mater. Chem* **2001**, *11*, 963–980.
(11) Cooper, D. W. *Part. Sci. Technol.* **1989**, *7*, 371–378.
(12) Attia, Y. A.; Ahmed, M. S.; Zhu, M. *Sol-Gel Processing*; Attia, Y. A., Ed.; Plenum Press: New York, 1994; p 311.
(13) Pajonk, G. M. *App. Catal.* **1991**, *72*, 217–236.
(14) Hrubesh, L. W.; Pekala, R. W. *Sol-Gel Processing and Applications*; Plenum Press: New York, 1994; p 363.
(15) Rolison, D. R. *Science* **2003**, *299*, 1698–1701.
(16) Hrubesh, L. W. J. *Non-Cryst. Solids* **1998**, *225*, 335–342.
(17) Chang, H. J.; Lu, C. Z.; Wang, Y.; Son, C.-S. *J. Korean Phys. Soc.* **2004**, *45*, 959–962.
(18) Bouguerra, M.; Samah, M.; Belkhir, M. A.; Chergui, A.; Gerbous, L.; Nouet, G.; Chateigner, D.; Madelon, R. *Chem. Phys. Lett.* **2006**, *425*, 77–81.
(19) He, H.; Wang, Y.; Zou, Y. *J. Phys. D: Appl. Phys.* **2003**, *36*, 2972–2975.
(20) Chakrabarti, S.; Ganguli, D.; Chaudhuri, S. *J. Phys. D: Appl. Phys.* **2003**, *36*, 146–151.
(21) Gash, A. E.; Tillotson, T. M.; Satcher, J. H.; Hrubesh, L. W.; Simpson, R. L. *J. Non-Cryst. Solids* **2001**, *285*, 22–28.
(22) Chervin, C. N.; Clapsaddle, B. J.; Chiu, H. W.; Gash, A. E.; Satcher, J. H., Jr.; Kauzlarich, S. M. *Chem. Mater.* **2006**, *18*, 1928–1937.
(23) Meador, M. A. B.; Fabrizio, E. F.; Ilhan, F.; Dass, A.; Zhang, G.; Vassilaras, P.; Johnston, J. C.; Leventis, N. *Chem. Mater.* **2005**, *17*, 1085–1098.

10.1021/cm0718419 CCC: $37.00
Published on Web 11/08/2007

Table 1. Summary of Synthetic Conditions for the Synthesis of ZnO Gels ([$Zn(NO_3)\cdot 6H_2O$] = 0.8 mmol; PO = 8 mmol; Solvent = 1.25 mL)

aerogel type	xerogel type	solvent	t_{gel} (h)
		water	no gel
A1	**X1**	methanol	8–10
A2	**X2**	ethanol	5–7
A3	**X3**	2-propanol	2–3
A4	**X4**	acetone	5–7

One of the advantages of the "epoxide addition method" is that it utilizes simple metal salts (i.e., metal nitrates or halides) instead of alkoxide precursors. As a result, novel aerogel materials can be prepared.[24–26] Here, we use the epoxide addition sol–gel process to synthesize monolithic zinc oxide aerogels and their xerogel analogues. The method presented is low-cost, versatile, and requires relatively few steps to produce ZnO-based porous materials.

Experimental Section

Synthesis of ZnO Gels. The reactants used in this preparation, $Zn(NO_3)\cdot 6H_2O$ (J.T. Baker), methanol (HPLC grade, Fisher), ethanol (100% reagent alcohol, Fisher), 2-propanol (HPLC grade, Fisher), acetone (ACS grade, Mallinckrodt), and propylene oxide (AlfaAesar) were used as received without further purification. Purified water was used from an ultrapure water system (Easy Pure II, Barnstead International). All syntheses were performed under ambient conditions.

In a typical synthesis, $Zn(NO_3)\cdot 6H_2O$ (0.8 mmol, 0.238 g) was dissolved in solvent (1.25 mL) and stirred to give a clear colorless solution. Subsequently, propylene oxide (8 mmol, 0.465 g) was added to the solution. The mixture was rapidly stirred for 2 min and transferred to a plastic mold, and the solution was allowed to gel undisturbed.

Following gelation, the gels were aged for 3–5 days under ambient conditions in closed vials to improve the firmness and robustness of the gel. The aged gels were then washed with acetone for ~1 week, with fresh acetone exchanged daily. Aerogel samples were processed in a SPI-DRY model critical point dryer. The acetone exchanged gels were transferred to the critical point dryer, where the acetone was exchanged with liquid CO_2(l) for 2–4 days, after which time the temperature of the vessel was ramped up to 45 °C and pressure above 1150 psi. Once the critical point was achieved, the critical point drier was depressurized over a period of 3 h to obtain monolithic aerogels. Xerogel samples were processed by slow evaporation of the acetone exchanged gels over a period of 30 days.

For the calcination studies the aerogels were heated to 150 and 250 °C with a ramp rate of 1 °C/min, and the temperature was maintained for 5 h, before returning to room temperature at 1 °C/min.

Physical Characterization. A Nova 3200e model surface area analyzer (Quantachrome Instrument Corp.) was used to obtain nitrogen physisorption isotherms at 77 K. Surface areas were evaluated using the Brunauer–Emmett–Teller (BET) method from the adsorption branch of the isotherm. The pore-size distributions were according to the Barrett–Joyner–Halenda (BJH) model, and the average pore diameters and cumulative pore volumes were calculated using the desorption branch of the isotherm. Before each set of measurements, the samples were degassed for 20–40 h. Each measurement took around 24 h to complete with a 150 s equilibrium interval.

The morphology and elemental distribution of the materials were studied by scanning electron microscopy (SEM) combined with energy dispersive X-ray (EDX) analysis using a Hitachi S-4300 scanning electron microscope. Accelerating voltages used for samples were 3 kV. Powder X-ray diffraction data were collected on aerogel samples using a Philips Nerelco diffractometer with an analyzing crystal. Cu Kα radiation was used, and samples were mounted on an aluminum plate. The photoluminescence (PL) emission spectra were obtained using a Fluoromax-3 spectrofluorometer (Jobin Yvon, Horiba) at 325 nm.

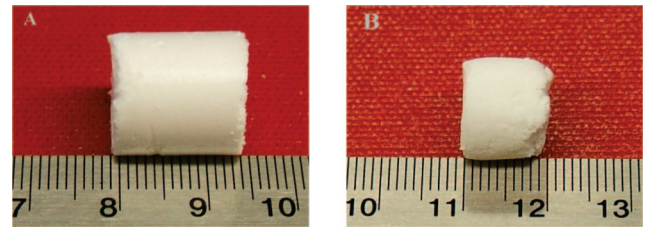

Figure 1. Photographs of monolithic as-synthesized ZnO aerogels: (A) using $Zn(NO_3)_2\cdot 6H_2O$ in methanol; (B) $Zn(NO_3)_2\cdot 6H_2O$ in ethanol.

Results and Discussion

Gel Formation Studies. White ZnO gels were prepared through the simple addition of propylene oxide to a solution of zinc nitrate. Soon after addition of the propylene oxide, the colorless solution became gradually cloudy before eventually becoming white. A summary of the various synthetic conditions used to prepare ZnO gels is shown in Table 1.

Successful gel formation was observed with all solvents investigated with the exception of water. The only significant differences observed appeared to be the gel times, which appear to be dependent on the identity of the solvent. For example, the gel time for the synthesis in methanol is 8–10 h whereas that for 2-propanol is significantly shorter with a gel time of 2–3 h. We attribute this to the differences in solubility and stability of zinc oxide sol in the various solvents.[21]

Gels shown in Table 1 were dried under atmospheric or supercritical conditions with CO_2(l) to produce xerogel and aerogel monoliths, respectively. Figure 1 contains photographs of monolithic as-prepared ZnO aerogel samples. Previous attempts to form stable aerogel monoliths from divalent transition metal salts, with the exception of nickel, have failed via the epoxide addition method.[21,25] This can be attributed to several factors, including metal acidity, low initial metal salt concentration, and insufficient epoxide-to-metal ratio to drive the reaction through to gelation. This postulation is based primarily on our initial work with zinc salts in which precipitation rather than gelation was always observed when the metal to epoxide mole ratio was lower than 6:1. The densities of the as-synthesized aerogels were calculated by determining the mass/volume ratio. For all aerogel materials regardless of reaction solvent the density was calculated to be ~0.04 g/cm^3. It should also be noted that

(24) Gash, A. E.; Tillotson, T. M.; Satcher, J. H.; Poco, J. F.; Hrubesh, L. W.; Simpson, R. L. *Chem. Mater.* **2001**, *13*, 999–1007.
(25) Gash, A. E.; Satcher, J. H.; Simpson, R. L. *J. Non-Cryst. Solids* **2004**, *350*, 145–151.
(26) Chervin, C. N.; Clapsaddle, B. J.; Chiu, H. W.; Gash, A. E.; Satcher, J. H., Jr.; Kauzlarich, S. M. *Chem. Mater.* **2006**, *18*, 4865–4874.

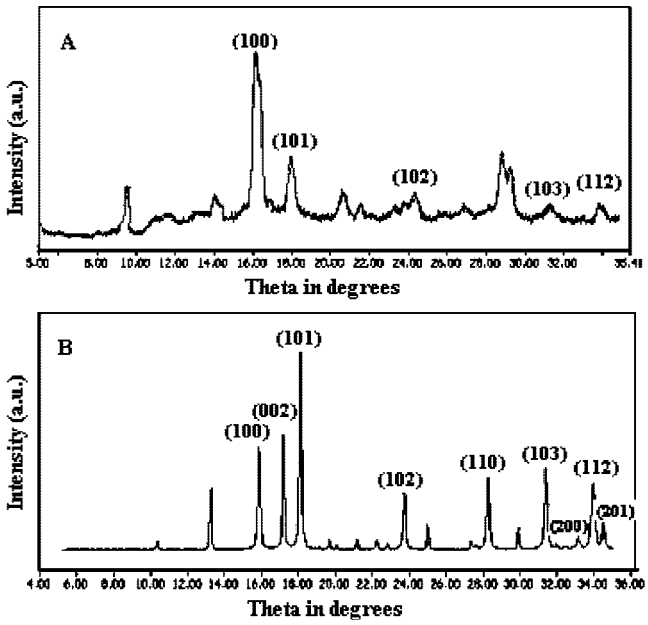

Figure 2. Powder X-ray diffraction patterns of zinc-based aerogels: (A) as-symthesized zinc aerogel, **A1**; (B) aerogel **A1**, annealed at 150 °C.

the stability of the resultant aerogel material was highly dependent on the reaction solvent. For example, ethanol, 2-propanol, and acetone were determined to not be suitable solvents for the formation of monolithic Zn(II) aerogels. The resultant products (**A2**, **A3**, and **A4**) were very fragile, and removal of the monoliths from their molds resulted in a significant amount of fracturing of the material, as shown in Figure 1B. The xerogel analogues, formed via ambient temperature drying by slow evaporation (~30 days) of the acetone-washed gels, resulted again in monolithic materials which retained the shape of the vial, with volume shrinkage of ~10% observed in all materials. Again the more robust monoliths were formed from methanol and could be readily removed from the vials in which they were cast.

The powder X-ray diffraction pattern of the as-prepared zinc aerogel **A1**, as shown in Figure 2A, contained a set of broad peaks, which can be matched to the (100), (101), (102), (103), and (112) lattice planes of wurtzite zinc oxide (JCPDS # 5-664). However, it is clearly evident that there is a significant amount of amorphous material also present in the as-synthesized aerogel. To increase the degree of crystallinity, the aerogel was annealed at 150 °C for 5 h, as shown in Figure 2B. The annealed highly crystalline aerogel correlates with all the major peaks assigned to the wurtzite zinc oxide phase. The diffraction peaks sharpen with better signal-to-noise ratio, corresponding to bigger particles of hexagonal ZnO. All other peaks are due to minor by products present in the aerogel samples.

The high-resolution scanning electron microscopy (HRSEM) results indicate the zinc oxide gels are particulate gels largely comprised of platelets. The macroscopic morphology differences between **A1** and **X1** are shown in Figure 3A,B. The morphology of the as-prepared aerogel **A1** appears to be composed of individual thin flakes, which cluster together to give a "flower"-like structure that contain cavities of mesoporous dimensions. The thin flake microstructure of **A1** is clearly evident in the high-magnification image inset in Figure 3A. The analogous xerogel **X1**, as shown in Figure 3B, appears to be composed of thin platelets with defined hexagonal shape, which are networked together to form large aggregates. The average platelets size is in excess of 500 nm, which is clearly seen in the high-magnification image inset in Figure 3B. The micrograph in Figure 3C is a low-magnification image of **A1** annealed at 150 °C that reveals the extended porous structure of the aerogel. As shown in the high-magnification image inset in Figure 3C, the aerogel annealed at 150 °C appears to be composed of defined hexagonal clusters, with the average cluster size below 400 nm in diameter. The analogous annealed xerogel of **X1**, shown in Figure 3D with the high-magnification image inset, appears to be very similar to the unheated xerogel. However, the high-magnification image shows a significant growth in the platelet size.

The EDX measurements on **A1** and **X1** were randomly performed on several spots across the samples. By this method the zinc-to-oxygen ratio was determined to be approximately stoichiometric, with the oxygen slightly in excess. This is probably due to the large degree of amorphousness present in the samples and the reaction byproducts. Additionally, the presence of minor amounts of carbon and nitrogen were also detected. These can also be attributed to the presence of residual organic by products which were not removed during the washing process.

Table 2 summarizes the surface areas, pore volumes, and average pore sizes for **A1**, **X1**, and the analogous annealed materials. Overall, the materials listed in Table 2 exhibited high surface areas and pore diameters in the mesoporic region. The xerogel **X1** has a comparable surface area to that of the aerogel **A1**, with the only noticeable difference being an increase in pore volume observed in the xerogel compared to the aerogel (0.30 cm^3/g compared to 0.17 cm^3/g, respectively). This is most likely a reflection of the difference in the gel morphology. The analogous annealed materials exhibited significantly smaller surface areas compared to the original materials, 277 m^2/g compared to 102 m^2/g for the aerogel-based material. In both cases there is minimal change observed in the pore volume with a dramatic increase in average pore diameter observed; this is likely a consequence of the aggregation of particles into larger platelets. In all materials the surface areas observed are significantly higher than those previously reported for ZnO nanoparticles synthesized by mechanochemical processing.[27]

The room temperature photoluminescence of the annealed aerogels, **A1**, was measured and shown in Figure 4. Two luminescence bands, including a strong near band-edge UV emission at ~396 nm and a blue emission at 469 nm, were observed. The weak yellow band usually observed in ZnO materials just above 600 nm was not observed. The UV emission is usually accredited to the direct recombination of excitons, through an exciton–exciton collision process. The other peak in the visible region is usually attributed to

(27) Aghababazadeh, R.; Mazinani, B.; Mirhabibi, A.; Tamizifar, M. *J. Phys.: Conf. Ser.* **2006**, *26*, 312–314.

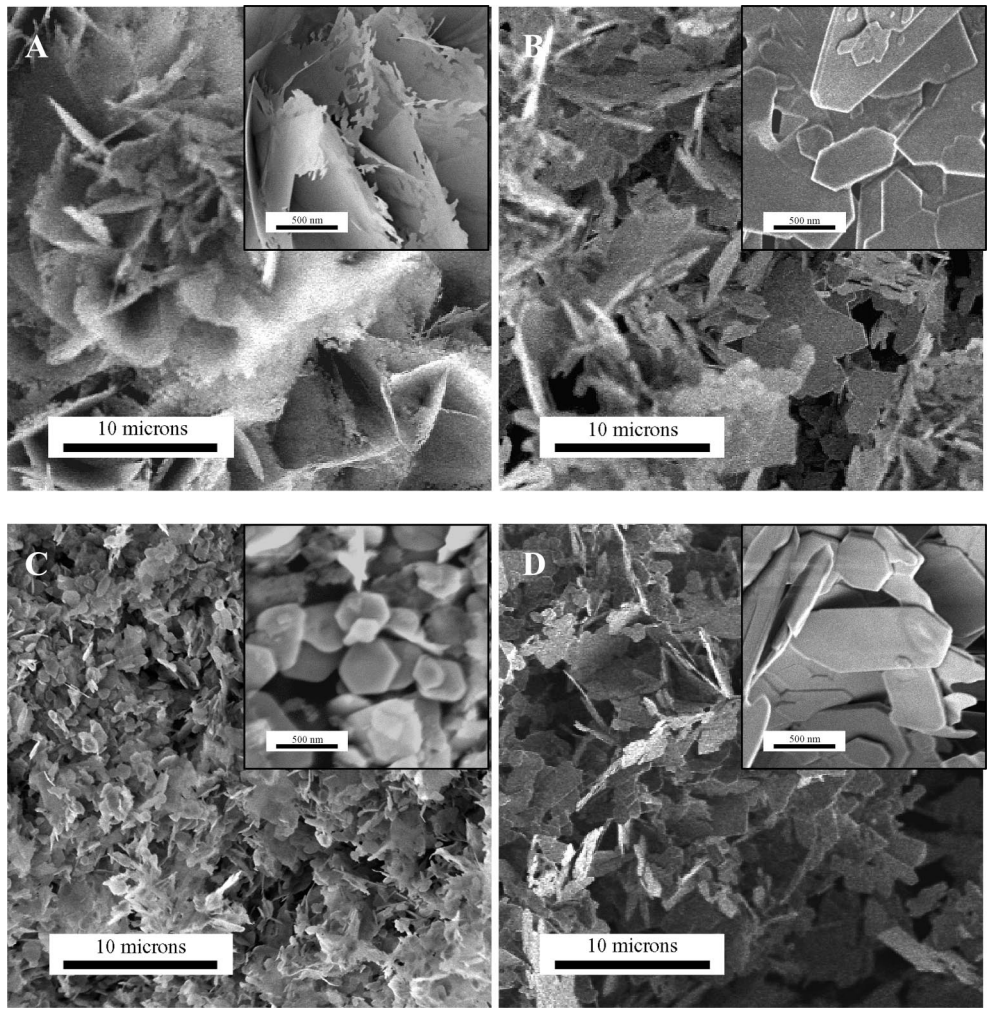

Figure 3. High-resolution scanning electron microscopy of (A) aerogel **A1**, (B) zinc oxide aerogel **X1**, (C) aerogel, **A1**, annealed at 150 °C, and (D) xerogel, **X1**, annealed at 150 °C.

Table 2. Physical Properties of Zinc Oxide Aerogels and Xerogels before and after Annealing

gel type	BET surface area (m^2/g)	BJH pore volume (cm^3/g)	BJH av pore radius (Å)
A1	277	0.17	15.4
X1	240	0.30	15.8
A1 at 150 °C	102	0.18	29.9
X1 at 150 °C	95	0.24	25.6

an internal defect emission, probably due to oxygen and zinc vacancies in the structure.[27–29]

The as-synthesized aerogel, **A1**, exhibited only weak emission peaks, which can be attributed largely to the highly amorphous nature of the unheated sample and small crystallite size. The PL spectrum of the sample annealed at 250 °C (dotted line) exhibits observed strengthening in the emission intensity of both the UV and blue emissions, which is likely due to the increased crystalline nature of the annealed samples as revealed by the XRD analysis.

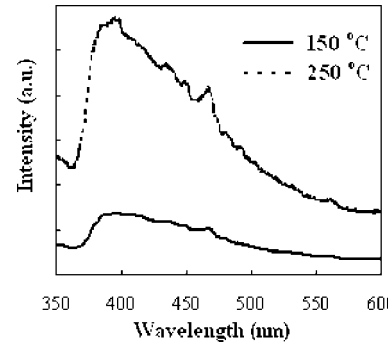

Figure 4. Photoluminescence spectra of annealed zinc aerogel, **A1**, at 150 and 250 °C (excitation $\lambda = 325$ nm).

Conclusion

In summary, on the basis of the epoxide sol–gel method and subsequent thermal processing steps, we have synthesized zinc oxide aerogels and xerogels for the first time, which exhibit high surface areas (>270 m^2/g), low densities (~0.04 g/cm^3), and significant porosity. The as-synthesized aerogel is composed of thin flakes arranged to give "flower"-like morphology, while the analogous xerogel is formed from hexagonal platelets networked together. Annealing treatment

(28) Cao, H.; Zhao, Y. G.; Ong, H. C.; Ho, S. T.; Dai, J. Y.; Wu, J. Y.; Chang, R. P. H. *Appl. Phys. Lett.* **1998**, *73*, 3656.
(29) Zhang, W.-H.; Shi, J.-L.; Wang, L.-Z.; Yan, D.-S. *Chem. Mater.* **2000**, *12*, 1408–1413.
(30) Xiong, H.-M.; Liu, D.-P.; Xia, Y.-Y.; Chen, J.-S. *Chem. Mater.* **2005**, *17*, 3062–3064.

of the as-synthesized aerogel materials results in a dramatic morphology change with the presence of hexagonal platelets clearly seen. The extended porous structure is preserved in the annealed samples while the measured surface is significantly reduced. Additionally, the annealed aerogels exhibit a dramatic enhancement of the UV and visible emission intensity due to the increased crystalline nature of the material. The ability to prepare ZnO-based porous materials through a simple sol–gel method presents a straightforward and cost-effective method for the design of new porous ZnO nanoarchitectures for a wide range of future applications.

CM0718419